Local smoothing in sandpiles: Spanning avalanches, bifurcation, and temporal oscillations

M. N. Najafi and Z. Moghadam*
Department of Physics, University of Mohaghegh Ardabili, P.O. Box 179, Ardabil, Iran

(Received 5 July 2018; published 15 April 2019)

The manipulation of the self-organized critical systems by repeatedly deliberate local relaxations (local smoothing) is considered. During a local smoothing, the grains diffuse to the neighboring regions, causing a smoothening of the height filed over the system. The local smoothings are controlled by a parameter ζ which is related to the number of local smoothening events in an avalanche. The system shows some new (mass and time) scales, leading to some oscillatory behaviors. A bifurcation occurs at some ζ value, above which some oscillations are observed for the mean number of grains, and also in the autocorrelation functions. These oscillations are associated with *spanning avalanches* which are due to the accumulation of grains in the smoothed system. The analysis of the rare event waiting time confirms also the appearance of a new time scale.

DOI: 10.1103/PhysRevE.99.042120

I. INTRODUCTION

The critical-state dynamics of avalanches has been the center of attention since the advent of the self-organized critical (SOC) systems [1–3]. Sandpiles, as the prototype of SOC systems, are slowly driven and evolve (without tuning of any external parameter) toward a steady critical state which is characterized by long-range spatial correlations and power-law behaviors. The nonlinearity of this model arises from a threshold value in such a way that when the local number of grains in some point of the system exceeds the threshold, the grains start to spread throughout the sample. Some experiments which are based on this idea show such nonlinearities. An example is in Ref. [3] which tested this model on realistic sandpiles at the angle of repose. The dynamics of the resulting avalanches is governed by the local updates (relaxations) depending on the state of sites at the moment, i.e., a domino effect (chain of relaxations) runs over the system which is mainly affected by the *minimally stable sites* (MSS) [1]. The latter (MSSs) are defined as the sites which become unstable under a single stimulation, i.e., adding a grain. The cluster comprised of MSSs is determinative for the dynamics of the underlying avalanche. When this cluster is very dense, i.e., the number of MSSs is high, the signal (caused by local stimulation) propagates throughout the sample and spans nearly the whole the system. Under the overall evolution of the system, other sorts of stable sites (i.e., more-than-minimally stable sites) appear at an increasing rate, which impede the propagation of the signal. In the steady state, the MSS cluster becomes dilute such that most signals are not spanning, i.e., signals become finite range [1]. In this case, the added grains are accumulated in the system, causing some large-scale (rare) events during which a large amount of grains leave the system. The diluted structure of the MSS cluster induces some critical behaviors which are reflected in power-law behaviors [2], and also conformal invariance [2], etc. The connection of the system in the critical state to the other statistical models is well understood and well studied. Examples are the connection with the spanning trees [4], the ghost models [4], and the q-state Potts model [5]. For a good review, refer to [2].

The relation of the sandpiles to natural phenomena, such as earthquakes [6], fluid propagation in reservoirs [7], and neuronal activities [8], makes the characterization of their critical dynamics worth studying. One output of such a study may be understanding and controlling the rare (large-scale) events. Importantly one may ask what the response of avalanches is to the external manipulation of the spatial distribution of grains or the propagation time scales. The example is the sticking effects of grains [9,10]. Another interesting curiosity to be addressed is the manipulation of the MSS cluster, i.e., how are the avalanches affected by the *hand-made changes* in the grain configuration in the MSS cluster? An example is the random relaxing of the MSS sites, under which one may hope that the spatial extent (range) of the avalanches decreases. This decrease is understood noting that every point on the MSS cluster can be considered as an agent who, when a signal is received, propagates (scatters) it symmetrically in $2d$ ($d \equiv$ the spatial dimension) directions. Relaxing MSSs means decreasing the abundance of these agents, which results in decreasing the range of the corresponding avalanche. In practice, however, the sandpiles due to their nonlinear structure, show richer structure with various behaviors under such a manipulation, and need a detailed simulation, which is the aim of the present paper.

We call such a local external relaxation *the local smoothing*. We control the strength of the local smoothings by a parameter, namely ζ, which is defined as follows: Suppose that after n_1 topplings, n_2 local smoothings (to be defined later) are applied, then $\zeta \equiv \frac{n_2}{n_1}$. Simply, when n_1 local topplings end, then n_2 local smoothings are applied. Actually we have seen that the results are independent of how this is arranged. Under applying local smoothings, the system shows some interesting nonlinear behaviors. We reveal that the avalanches are robust against applying the local smoothings (their

*zahramoghadam.physics@gmail.com

large-scale behaviors do not change considerably) up to a point (ζ^*) at which a bifurcation takes place and the system experiences a new regime within which some oscillations occur between two limits. Above ζ^*, along with the ζ-dependent oscillations of the grain number average, the autocorrelation functions also oscillate with some ζ-dependent frequencies. As ζ increases further, a new time scale in the rare event waiting time (REWT) appears and becomes dominant as ζ becomes larger than some threshold, i.e., $\zeta \gtrsim \zeta_c$.

Let us first define the model in a square $L \times L$ lattice in the $\zeta = 0$ limit, which is the ordinary Bak-Tang-Wiesenfeld (BTW) model. In this model, each site i has an integer height (the number of grains) $E_i \geqslant 1$. At the initial state, one can set randomly the height of each site with the restriction $E_i \leqslant E_c \equiv 4n$, in which n is an arbitrary integer, and is set to 10 in this paper. At each time step a grain (as a single stimulation) is added to a randomly chosen site ($E_i \to E_i + 1$). This can be considered as a slow external drive and leads to a fast relaxation process (avalanche) within the system. This relaxation consists of a conservative redistribution of the grains at the sites, i.e., if the height of a site exceeds E_c, then $E_i \to E_i + \Delta_{i,j}$ in which $\Delta_{i,j} = -E_c$ if $i = j$, $\Delta_{i,j} = n$ if i and j are neighbors, and zero otherwise. A toppling may cause the nearest-neighbor sites to become unstable (have a height larger than E_c) and topple in their own turn and so on, until all sites over the lattice are stable.

Now let us introduce the local smoothings. A local smoothing is defined as the action in which a site is chosen randomly and is checked for a more stable configuration. To do this, the height of its neighbors is checked. Suppose that the selected site is i with nearest neighbors i_1, i_2, i_3, and i_4. Among these neighbors, we label $i_{\max}$ as the site in which $E(i_{\max}) = \mathrm{Max}\{E_i\}_{i=1}^4$, and $i_{\min}$ as the site in which $E(i_{\min}) = \mathrm{Min}\{E_i\}_{i=1}^4$. A local smoothing is composed of two updates: $\delta E_1 \equiv \mathrm{int}\{[E(i_{\max}) - E(i)]/2\}$ grains (if positive) flow from the site $i_{\max}$ to i, and then $\delta E_2 \equiv \mathrm{int}\{[E(i) - E(i_{\min})]/2\}$ grains (if positive) flow from the site i to $i_{\min}$, in which int$[x]$ is the integer part of x. In the case of more than one site having the same (maximum or minimum) height, the site from or into which the grains flow is chosen randomly. If the site i is locally maximum (minimum), automatically no grain flows into (from) the site to the neighbors. No local smoothing is applied to the unstable sites. Therefore, we have two kinds of relaxation: the sites which are unstable topple and the sites which are chosen for local smoothings moderate their local height gradient. We call the first procedure as the *toppling* and the second one as the *local smoothing*. This problem can also be called a *diffusive sandpile model*, in which the grains are lubricated such that they have the chance to slip to the neighboring sites. The local relaxation in a fillip has been schematically shown in Fig. 1.

Let us consider the problem from another point of view. Applying local relaxations (local smoothings) means that the system is being smoothed and the number of MSSs decreases, i.e., the avalanches become lower in range, and the toppling events in the avalanches decrease. As a result, the number of grains that leave the system decrease, and accordingly, the balance between external drive and the dissipated grains is displaced. This cannot last for much time, since the average height of the system, which grows with the external drive, cannot become larger than $E_{\mathrm{th}} \equiv E_c$. In other words, when $\bar{E} \to E_{\mathrm{th}}$ under external drives, some very large avalanches take place. This can be understood noting that in this limit the number of MSSs is nearly close to L^2.

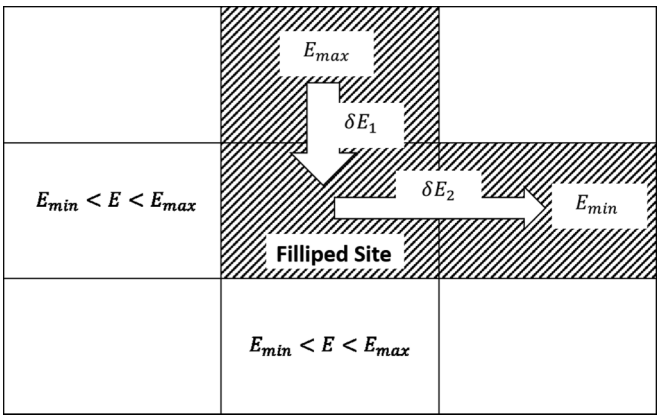

FIG. 1. Schematic of a fillip. The shaded sites are affected [δE_1 (δE_2) energy units transfer from (into) the site $i_{\max}$ ($i_{\min}$)] by the fillip. For the rules of the energy transfer (δE_1 and δE_2) refer to the text.

II. MEAN-FIELD ANALYSIS

The critical absorbing states in sandpiles are hyper-uniform with long-range spatial anticorrelations. Periodic perturbation to such a state could generate some temporal oscillations [11]. Let us consider the problem in the mean-field (MF) level. Consider a square lattice with $N = L^2$ sites and $4L$ boundary sites. Suppose that the avalanche mass (number of toppled sites in an avalanche) at time T had been $A(T)$, and one energy unit is added at $T + 1$, and also the average height at time T (Tth injection) is considered to be $\bar{E}(T)$. When one energy unit is added to the system, then the average energy is raised by $1/N$. But some energy is dissipated from the boundaries. In the mean-field level, we should first calculate the probability that a boundary site had been unstable in the previous avalanche. This probability is simply the number of boundary sites ($4L$) times the probability that a random chosen site is involved in the avalanche. The latter is equal to $A(T)/N$. All in all, we reach the following result for the time-dependent average energy:

$$\bar{E}(T+1) = \bar{E}(T) + \frac{1}{N} - 4L\frac{A(T)}{N}. \tag{1}$$

The above analysis reveals that in the steady state in which $\bar{E}(T+1) = \bar{E}(T)$, we have $\bar{A}(T) = \frac{1}{4L}$. Now consider the effect of local smoothing. We suppose that its effect is decreasing the range of the corresponding avalanches $A'(T)$, and also suppose that $A'(T)$ is proportional to $A(T)$ (the same avalanche in the absence of local smoothing). The proportionality constant is surely ζ dependent, i.e., $A'(T) = f(\zeta)A(T)$. In this case, under the conditions that the zero-smoothing $\zeta = 0$ system is in the steady state, we have

$$\bar{E}(T+1) = \bar{E}(T) + \frac{1}{N}[1 - f(\zeta)]. \tag{2}$$

This means that $\bar{E}$ grows linearly with time (with the proportionality constant $\frac{1}{N}[1 - f(\zeta)]$. This growing takes place up to

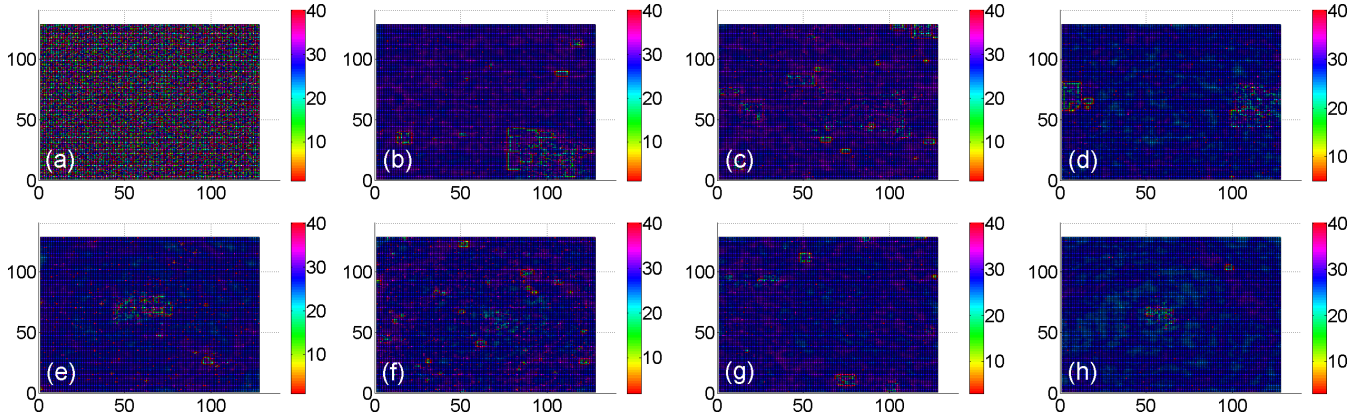

FIG. 2. Generated 128×128 samples for $\zeta = 0$, $\zeta = 4$, $\zeta = 8$, $\zeta = 10$, $\zeta = 16$, $\zeta = 24$, $\zeta = 32$, and $\zeta = 48$ (from left to right and top to bottom).

a time that $\bar{E} \to E_{\rm th}$ at which the avalanche mass reaches the system size. In this case $A(T) \approx N = L^2$. In this case Eq. (1) shows that

$$\bar{E}(T+1) = \bar{E}(T) - (4L-1). \tag{3}$$

In this case the average energy decreases abruptly by $4L-1$. To continue, we introduce the probability of $\bar{E}(T+1) = z$, conditioned to $\bar{E}(T) = M$, which is found to be

$$P(\bar{E}_{T+1} = z | \bar{E}_T = M) = \begin{cases} \delta_{z,M+\frac{1}{N}(1-f(\zeta))} & M < E_{\rm th}, \\ \delta_{z,M-4L+1} & M \approx E_{\rm th}. \end{cases} \tag{4}$$

One of the important quantities in the analysis of the dynamical systems is the branching ratio defined by $b(M) \equiv \mathbf{E}[\frac{\bar{E}_{T+1}}{M} | \bar{E}_T = M]$. For a given M, if $b(M) > 1$ then the average $\bar{E}$ grows, and if $b(M) < 1$ then it decreases. The above calculations show that

$$b(M) = \begin{cases} 1 + \frac{1-f(\zeta)}{NM} & M < E_{\rm th}, \\ 1 - \frac{4L-1}{M} & M \approx E_{\rm th}, \end{cases} \tag{5}$$

in which $\mathbf{E}[\ ]$ is the expectation value. Note that when $b(M) > 1$ [$b(M) < 1$], then for a given M, the average number of grains of the system will increase (here linearly) (decrease, here abruptly) with T. This relation predicts that a bifurcation takes place at a nonzero ζ, above which some oscillations occur. For the first branch, the mean height increases linearly with T up to time at which $\bar{E} \approx E_{\rm th}$. At this point the average height drops abruptly by $\delta\bar{E} \approx -4L$ (the lower branch). This is accompanied with some large avalanches, which are named as *spanning avalanches* (SA). This dropping should be independent of ζ.

To test these predictions, we have calculated and plotted $\bar{E}$ in terms of T for various rates of ζ in Fig. 4(a). Two separate regimes are distinguishable in this figure: In the primitive times it increases linearly, and for large enough times it enters a new regime, e.g., for $\zeta = 0$ it is nearly constant. However, for nonzero ζ we see that some oscillations arise in which the average grain number drops abruptly after a linear part in accordance with the prediction of the MF approach. In the inset of this figure we have plotted the difference between these two limits (among which $\bar{E}$ oscillates) $\bar{E}_1 - \bar{E}_2$ in terms of ζ, which quantifies these oscillations. This figure characterizes the bifurcation point at which the transition to the oscillatory regime takes place. Actually $\bar{E}_1 - \bar{E}_2$ starts from zero in small enough ζ and at some L-dependent bifurcation point (ζ^*) grows rapidly, and then saturates

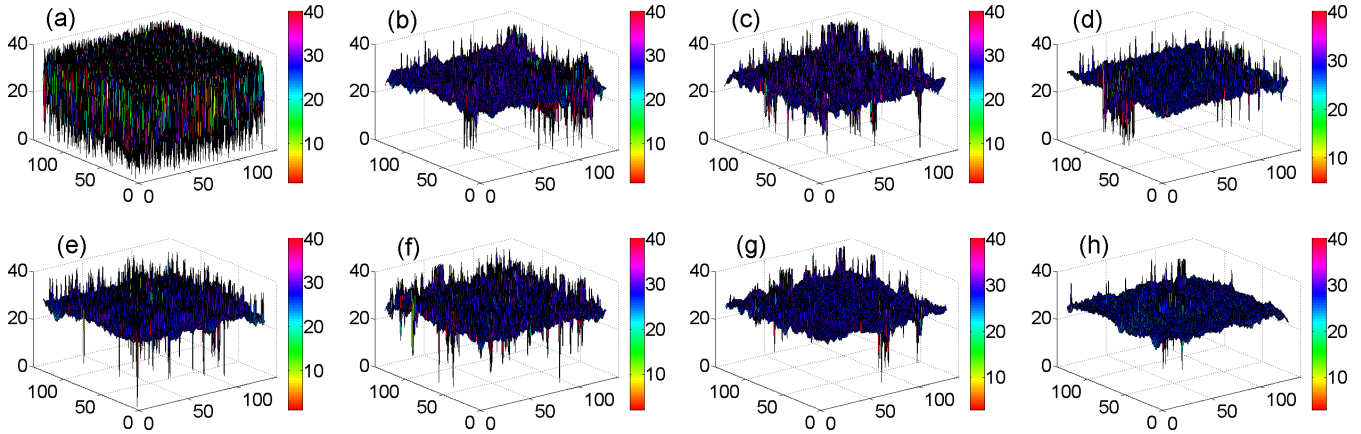

FIG. 3. : Roughness of the 128×128 samples for $\zeta = 0$, $\zeta = 4$, $\zeta = 8$, $\zeta = 10$, $\zeta = 16$, $\zeta = 24$, $\zeta = 32$, and $\zeta = 48$ (from left to right and top to bottom).

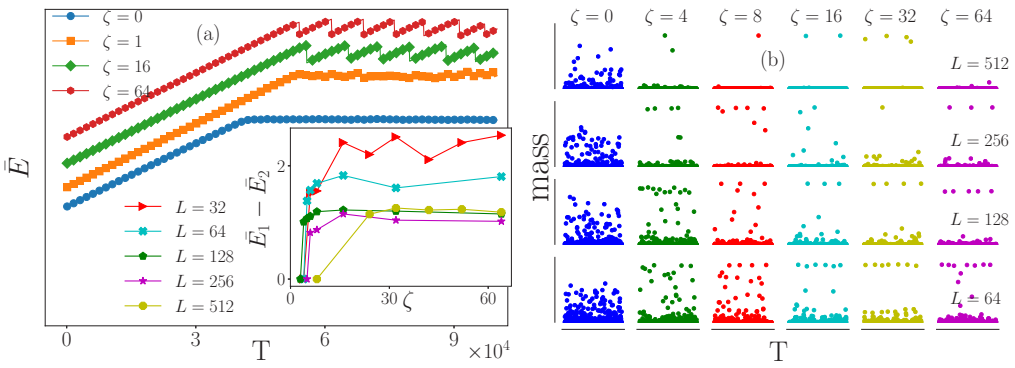

FIG. 4. (a) The (shifted) height average in terms of T (the number of injections) for various rates of ζ. Inset: $\bar{E}_1 - \bar{E}_2$ in terms of ζ. (b) Mass as a function of time T for various rates of ζ and L.

immediately. The fact that after the saturation, $\bar{E}_1 - \bar{E}_2$ becomes almost independent of ζ confirms the prediction of the MF calculations. We also have observed that ζ^* varies more or less linearly with $\log L$. In the following, we see that the physics of these two regimes are different.

III. NUMERICAL RESULTS

In the MF approach, we claimed that these oscillations are due to two branches in Eq. (5). In this section we present the numerical results. The samples have been shown in Figs. 2 and 3. It is seen that the configurations become smoother under the application of fillips.

Figure 4(b) visualizes this event, in which a new characteristic reference point appears for large enough ζ. In this figure we have shown the mass of the avalanches ($\equiv$ the number of distinct toppled sites in the avalanche) as a function of time for various rates of ζ and L. Consider for example $L = 64$ in the regime $\zeta \gtrsim 8$, for which the masses of some avalanches reach the system size, i.e., the top points in the figure whose mass is almost $(64)^2 = 4096$. These avalanches are the mentioned SAs, and are absent in small ζ. The SAs and the abrupt drop of average height occur simultaneously and therefore have the same origin [both belong to the lower branch of Eq. (5)]. The avalanches that belong to the first branch, whose mean sizes grow linearly with the injections are called *deformed avalanches* (DAs). The mean size of DAs depends on $E_{\rm th} - \bar{E}$.

It is notable that the microstates which grow with time in the observed *quasistationary state* are transient. The existence of transient states in the quasisteady state may lead to new studies, and new insights may come up for the phenomena of SOC as a whole.

Although these figures are helpful for understanding the phenomenon, some other tests are necessary to quantify it. The autocorrelation function of the mass noise $\{m(T)\}_{T=1}^{T_{\max}}$ [in which $m(T)$ is the mass of Tth avalanche, and $T_{\max}$ is the maximum T in our analysis] is defined as

$$f_{\rm mass}(T_0) \equiv \langle m(T)m(T+T_0)\rangle_T - (\langle m(T)\rangle_T)^2 \qquad (6)$$

in which the T average of an arbitrary statistical observable is defined by [12] $\langle O\rangle_T \equiv \frac{1}{T_{\max}}\sum_{T=0}^{T_{\max}} O[m(T)]$. Figure 5(a) shows the rescaled autocorrelation function of $m(T)$ defined by $A_{\rm mass}(T) \equiv [\langle m(T)\rangle_T]^{-2} f_{\rm mass}(T)$. Also the power spectrum (PS) is defined by $\mathrm{PS}_{\rm mass}(\omega) \equiv \lim_{T_{\max}\to\infty} \frac{1}{T_{\max}} \left| \int_0^{T_{\max}} dT\, m(T) \exp[-i\omega T] \right|^2$, and is proportional to the Fourier transform of $A_{\rm mass}(T)$. The same definitions hold also for the activity noise.

As is seen in Fig. 5(a), as ζ increases (more precisely for $\zeta \gtrsim 8$), some oscillatory behaviors appear. These oscillatory behaviors are due to the new reference point that was mentioned above. In other words, the oscillations in $\bar{E}(T)$ are responsible for this oscillatory autocorrelation. The most robust (long-range) oscillations are found for $\zeta \approx 16$ for $L = 256$. It

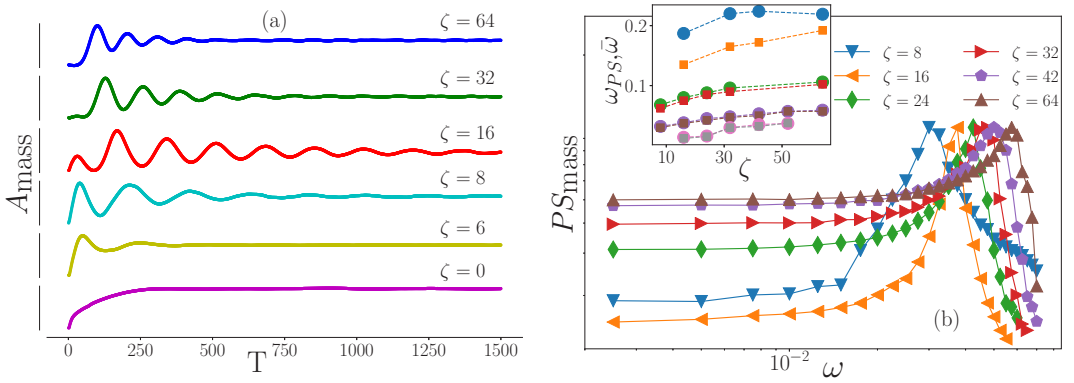

FIG. 5. (a) Time dependence of mass autocorrelation function ($L = 256$). (b) Mass power spectrum in terms of frequency. Inset: the peaks of PS (solid squares) and average frequencies of $\bar{E}$ (solid circles) for $L = 32$, 64, 128, and 256 (from top to bottom).

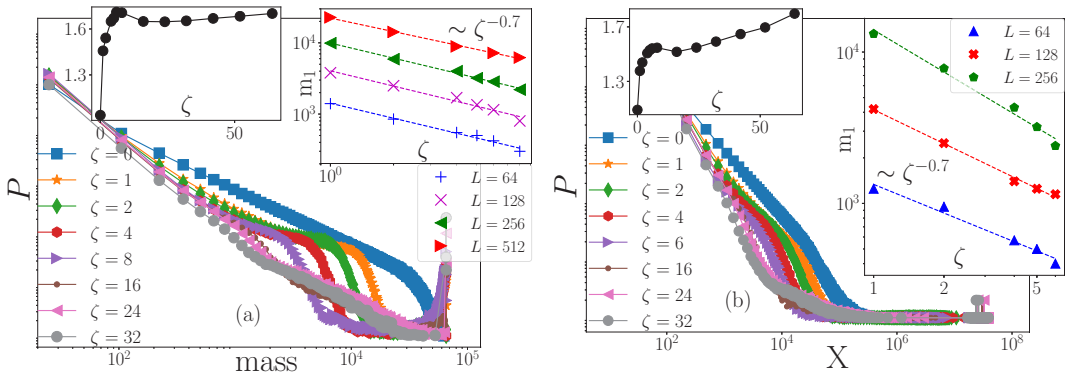

FIG. 6. Distribution of the (a) mass and (b) activity. Left insets: the slope of the first part of the graphs. Right insets: the power-law behavior of m_1.

is notable that these ζ values are L dependent. To strengthen the connection of these oscillations and the oscillations for $\bar{E}(T)$, one should calculate the power spectrum of the noise (here the mass) and find its peak. The resulting frequencies can then be compared with the frequencies of the oscillations of $\bar{E}(T)$. This is done in Fig. 5(b) for $L = 256$. For small ζ values ($\zeta = 2$ in this figure), one finds no peak, whereas for larger ζ a peak appears which runs with ζ. In the inset, the position of these peaks (ω_{PS}, the solid squares) has been shown for some lattice sizes, along with the average angular frequency ($\bar{\omega}$) obtained from the oscillations of $\bar{E}(T)$ (the solid circles). The fact that these frequencies are properly matched shows that they have the same origin, i.e., the system oscillates between two states: DAs and SAs. These frequencies increase monotonically with ζ, revealing that the local smoothings facilitate the creation of the SAs. The distribution functions have also the capability to reflect the status of the system in hand (Fig. 6), which should be power law for $\zeta = 0$ [Fig. 6(a)]. However for nonzero ζ they change considerably, especially a new mass scale (namely, m_1) comes into play

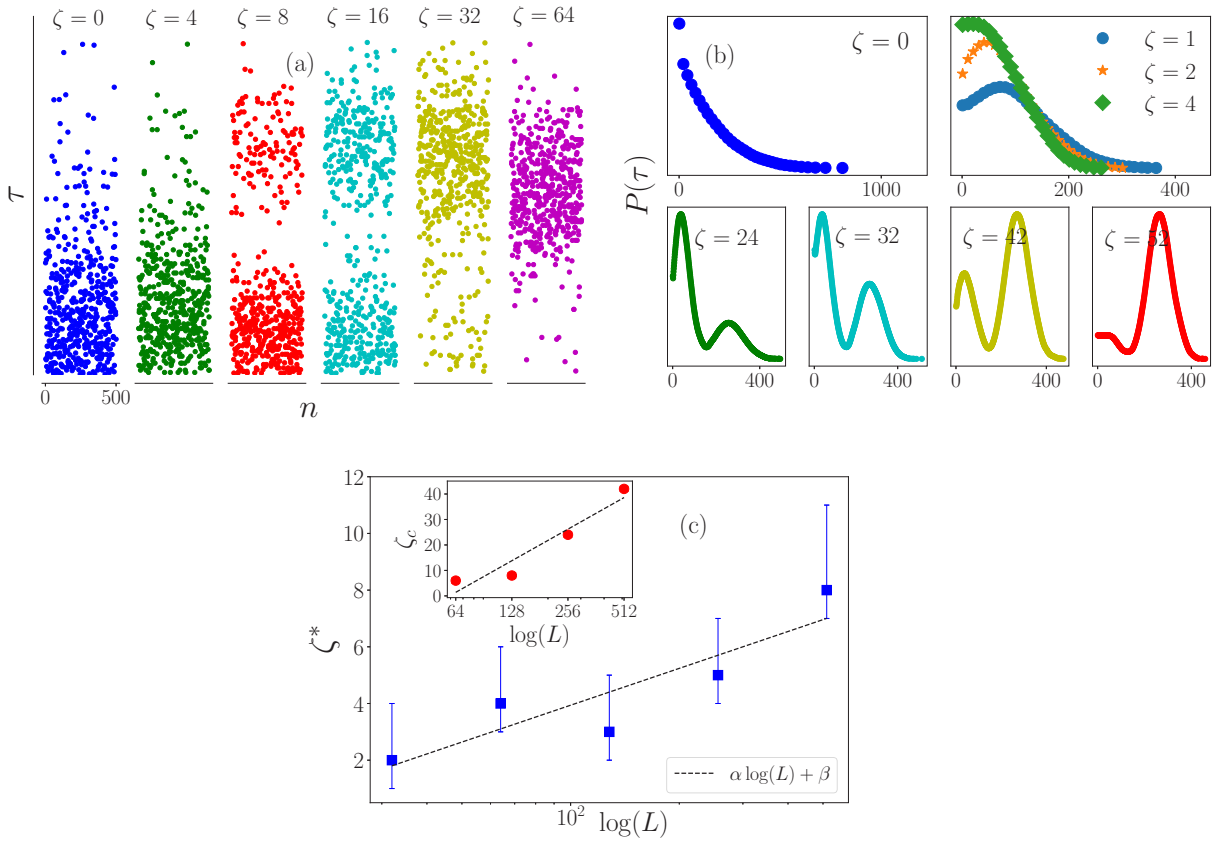

FIG. 7. (a) Time series of REWT and (b) its corresponding distribution with a new time scale. (c) The semi-log plot of ζ^* and ζ_c as a function of system size, suggesting that $\zeta^*, \zeta_c = \alpha \ln L + \beta$ in which $\alpha = 1.9 \pm 0.3$ for ζ^*, and $\alpha = 17.9 \pm 2.0$ for ζ_c. Note that $\alpha_{\zeta^*} < \alpha_{\zeta_c}$.

below which the linearity of the log-log graph is retained. The slope of the graphs in small masses has been shown in the left inset of this graph. Also a sharp peak is seen at mass $= 65536 = (256)^2$, which are SAs in accordance with the above calculations. A more precise look at this figure reveals that m_1 decreases (in a power-law fashion) with increasing ζ up to some ζ_c (≈ 16 for $L = 256$). The same features are seen for the distribution of the activity $P(X)$ [Fig. 6(b)].

To uncover the physics of ζ_c we need to investigate the REWT. The REWT, which has deep connections with the kind of activity noise, is defined as the waiting time between two large avalanches, i.e., the avalanches with sizes larger than a threshold value $s_{\text{threshold}}$ (as a large event) which is fixed to be $2L^2$ here. We have observed that our results are more or less independent of the exact value of this threshold. We define REWT, denoted by $\tau(n)$, as the time interval between two successive rare events $s(T_n)$ and $s(T_{n+1})$. In other words if the (n)th rare event occurs at time T_n [i.e., $s(T_n) > s_{\text{threshold}}$] and the next rare event occurs at time T_{n+1}, then $\tau(n) \equiv T_{n+1} - T_n$. Figures 7(a) and 7(b) show the results for REWT for $L = 256$. It is interestingly seen from Fig. 7(a) that for $8 \lesssim \zeta \lesssim 16$ the aggregation of events is in two reference points, i.e., the corresponding distribution functions are doubly peaked, whereas for $\zeta \lesssim 8$ they are singly peaked. This can be better seen in Fig. 7(b), in which the lower graphs correspond to $\zeta > 8$. We see that as ζ increases, the second peak grows, whereas the first one weakens. If we show the amount of ζ at which the abundance of these two peaks becomes the same by ζ_c, then we interestingly see that this ζ_c coincides with the ζ scale up to which m_1 behaves as a power law in Figs. 6(a) and 6(b). For $\zeta \gtrsim \zeta_c$ we expect that a new characteristic τ governs the system. In Fig. 7(c) we have shown ζ^* and ζ_c in terms of system size L, which is best fitted to a logarithmic function. Although both ζ^* and ζ_c diverge in the thermodynamic limit, for any finite L we observe two crossovers as ζ is increased, first to an oscillatory phase and then to a regime with a new time scale in REWT.

IV. CONCLUSION

By *smoothing* (applying local smoothings on) the BTW system, the system meets various regimes and various new characteristic scales. For $0 \leqslant \zeta \lesssim \zeta^*$, although the range of avalanches decrease with ζ (see Fig. 6 in which the abundance of large avalanches is lower than that of $\zeta = 0$ avalanches), but no oscillations are found. These oscillations are also reminiscent of quasiperiodic events in crystal plasticity [13]. In this interval a new mass scale (m_1 in Fig. 6 which decreases in a power-law fashion with ζ) is found which corresponds to the new τ scale in Fig. 7(b). A bifurcation takes place in $\zeta = \zeta^*$, in such a way that for $\zeta^* \lesssim \zeta \lesssim \zeta_c$ some long-range oscillations are found [Fig. 5(a)]. As ζ increases further, for $\zeta_c \lesssim \zeta$, $\bar{E}_1 - \bar{E}_2$ [Fig. 4(a)] as well as the mass scale m_1 (Fig. 6) saturate. At this interval a new τ scale appears and grows with ζ [Fig. 7(b)]. It is notable that these thresholds are L dependent and for $L = 256$, $\zeta^* \approx 8$ and $\zeta_c \approx 35$.

According to these findings the attempt to smooth a sandpile causes the system to meet some unexpected regimes. This smoothening may be translated to some deliberate artificial bursts in the avalanches of natural SOC systems (e.g., artificial earthquakes in the real earthquakes). Our calculations demonstrate that this causes some energies to accumulate in the system, leading to spanning avalanches and oscillatory behaviors.

[1] P. Bak, C. Tang, and K. Wiesenfeld, Phys. Rev. Lett. **59**, 381 (1987).
[2] D. Dhar, Physica A **369**, 29 (2006).
[3] H. M. Jaeger, C.-h. Liu, and S. R. Nagel, Phys. Rev. Lett. **62**, 40 (1989).
[4] S. N. Majumdar and D. Dhar, Physica A: **185**, 129 (1992).
[5] H. Saleur and B. Duplantier, Phys. Rev. Lett. **58**, 2325 (1987).
[6] A. Sornette and D. Sornette, Europhys. Lett. **9**, 197 (1989).
[7] M. N. Najafi, M. Ghaedi, and S. Moghimi, Physica A **445**, 102 (2016).
[8] L. de Arcangelis, C. Perrone-Capano, and H. J. Herrmann, Phys. Rev. Lett. **96**, 028107 (2006).
[9] P. K. Mohanty and D. Dhar, Phys. Rev. Lett. **89**, 104303 (2002).
[10] P. K. Mohanty and D. Dhar, Physica A **384**, 34 (2007).
[11] R. Garcia-Millan, G. Pruessner, L. Pickering, and K. Christensen, Europhys. Lett. **122**, 50003 (2018).
[12] J. Davidsen and H. G. Schuster, Phys. Rev. E **62**, 6111 (2000).
[13] S. Papanikolaou *et al.*, Nature **490**, 517 (2012).